



CHORUS

This is the accepted manuscript made available via CHORUS. The article has been published as:

Twisted Hubbard Model for $\text{Sr}_{\{2\}}\text{IrO}_{\{4\}}$: Magnetism and Possible High Temperature Superconductivity

Fa Wang and T. Senthil

Phys. Rev. Lett. **106**, 136402 — Published 30 March 2011

DOI: [10.1103/PhysRevLett.106.136402](https://doi.org/10.1103/PhysRevLett.106.136402)

Twisted Hubbard Model for Sr_2IrO_4 : Magnetism and Possible High Temperature Superconductivity.

Fa Wang¹ and T. Senthil¹

¹*Department of Physics, Massachusetts Institute of Technology, Cambridge, Massachusetts 02139*

(Dated: January 13, 2011)

Sr_2IrO_4 has been suggested as a Mott insulator from a single $J_{\text{eff}} = 1/2$ band, similar to the cuprates. However this picture is complicated by the measured large magnetic anisotropy and ferromagnetism. Based on a careful mapping to the $J_{\text{eff}} = 1/2$ (pseudospin-1/2) space, we propose that the low energy electronic structure of Sr_2IrO_4 can indeed be described by a SU(2) invariant pseudospin-1/2 Hubbard model very similar to that of the cuprates, but with a “twisted” coupling to external magnetic field (a g -tensor with a staggered antisymmetric component). This perspective naturally explains the magnetic properties of Sr_2IrO_4 . We also derive several simple facts based on this mapping and the known results about the Hubbard model and the cuprates, which may be tested in future experiments on Sr_2IrO_4 . In particular we propose that (electron-)doping Sr_2IrO_4 can potentially realize high-temperature superconductivity.

PACS numbers: 71.10.Fd, 74.10.+v, 75.30.Gw

Various Ir oxides have recently become the platform to study the interplay between strong spin-orbit(SO) interaction and strong correlation effects. There has been an experimental observation of a three-dimensional spin liquid in a hyper-kagome structure of $\text{Na}_4\text{Ir}_3\text{O}_8$ [1]. Theoretical proposals such as the realization of correlated topological insulators [2], the Kitaev model [3], and a Dirac semimetal with surface “Fermi arcs” [4] in iridates have been made as well. Here we propose that doped Sr_2IrO_4 may realize high-temperature superconductivity similar to the cuprates.

The crystal structure of Sr_2IrO_4 consists of two-dimensional(2D) IrO_2 layers, similar to the parent compound La_2CuO_4 of the cuprates. The main difference is that the oxygen octahedra surrounding Ir rotate along c -axis by about 11° in a staggered pattern, enlarging the unit cell by $\sqrt{2} \times \sqrt{2} \times 2$ [5]. The electronic structure of Sr_2IrO_4 is quasi-2D, but is expected to have several differences from the cuprates. Ir^{4+} has the electronic structure $5d^5$, so the t_{2g} levels should be active, while Cu^{2+} with $3d^9$ configuration has only the top e_g level active. Ir as a $5d$ transition metal is expected to have weaker correlation effects than $3d$ elements(e.g. Cu). At this point one may expect that Sr_2IrO_4 is a (multi-band) weakly correlated metal. But strong spin-orbit coupling of Ir dramatically changes the story. The t_{2g} levels are split by SO interactions into a higher energy Kramers doublet (the pseudospin-1/2 or $J_{\text{eff}} = 1/2$ states) and two pairs of lower energy ones ($J_{\text{eff}} = 3/2$ states) [6]. These $J_{\text{eff}} = 1/2$ states are equal weight superpositions of all three t_{2g} orbitals, and this has been confirmed experimentally by resonant x-ray scattering [7] and theoretically by LDA+SO+U calculation [8]. With d^5 configuration of Ir the $J_{\text{eff}} = 1/2$ states are half-filled. They have much smaller band width than expected for the t_{2g} levels without SO interaction and therefore effectively enhanced correlation effect. In the end Sr_2IrO_4 is a Mott

insulator and exhibits magnetic order below 240K [9–11].

It is tempting to make the analogy between Sr_2IrO_4 and the cuprates and speculate that doped Sr_2IrO_4 can also realize the interesting physics in doped cuprates, e.g. superconductivity, pseudogap, stripe formation, etc.. But strong SO interaction, different active orbitals and the rotation of oxygen octahedra seem to significantly complicate the problem. For example, Sr_2IrO_4 has very anisotropic susceptibility and shows ferromagnetism(FM) with large ferromagnetic moment $\sim 0.14\mu_B$ per Ir [12], which was attributed to Dzyaloshinskii-Moriya(DM) interaction generated by the rotation of oxygen octahedra. However it has been pointed out by Jackeli and Khaliullin [3] that the DM interaction can be removed by staggered rotation of pseudospin spaces on Ir sites. We will extend this consideration to the electronic model and show that Sr_2IrO_4 can be approximately described by a SU(2) invariant one band Hubbard model under careful interpretation. The Hubbard model has a “twisted” coupling to external magnetic field, namely a g -tensor with staggered antisymmetric component. Except this fact the model of Sr_2IrO_4 remarkably resembles that of the cuprate. By making analogies to the cuprates we will propose that various interesting physics including high-Tc superconductivity may be realized in Sr_2IrO_4 . Our formulation provides a simplified picture (despite the complicated structure, strong SO coupling and nontrivial magnetism) for the electronic structure of Sr_2IrO_4 , and hopefully some guide for future experimental researches.

The mapping to one band Hubbard model. To begin with we will treat Sr_2IrO_4 as quasi-2D and consider only one IrO_2 layer, which is schematically illustrated in Fig. 1. Label the rotation angle of oxygen octahedron around Ir site j by $\theta_j = \epsilon_j\theta$, with $\epsilon_j = \pm 1$ for the two sublattices and $\theta \approx 11^\circ$ from experiments [5]. The crystal-field splitting of t_{2g} and e_g levels and projection

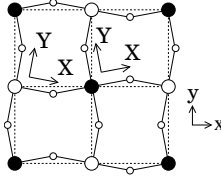


FIG. 1: Schematic picture of one IrO_2 layer. Large filled/open circles indicate the Ir atoms on two sublattices. Small open circles are oxygens. Small x, y are the global axis, while capital X, Y indicate local cubic axis(sublattices dependent).

to $J_{\text{eff}} = 1/2$ states should be implemented in the rotated local cubic axis. Label the global axis by x, y, z and local cubic axis (on site j) by X, Y, Z (see Fig. 1). The unit vectors of these two coordinates systems are related by

$$\hat{X} = \hat{x} \cos \theta_j + \hat{y} \sin \theta_j, \quad \hat{Y} = -\hat{x} \sin \theta_j + \hat{y} \cos \theta_j, \quad \hat{Z} = \hat{z}. \quad (1)$$

The $J_{\text{eff}} = 1/2$ states are (see e.g. Ref. [6], the phase convention here is slightly different, $\mathbf{i} = \sqrt{-1}$)

$$\begin{aligned} |J_{\text{eff}}^z = +1/2\rangle &= \frac{1}{\sqrt{3}} (+\mathbf{i}|XY, \uparrow\rangle - |XZ, \downarrow\rangle + \mathbf{i}|YZ, \downarrow\rangle), \\ |J_{\text{eff}}^z = -1/2\rangle &= \frac{1}{\sqrt{3}} (-\mathbf{i}|XY, \downarrow\rangle + |XZ, \uparrow\rangle + \mathbf{i}|YZ, \uparrow\rangle). \end{aligned} \quad (2)$$

XZ, YZ, XY are the t_{2g} orbitals defined in the *local* cubic axis. \uparrow, \downarrow indicate spin states (defined also in the *local* cubic axis). Note that although the elongation of oxygen octahedra along c -axis is expected to change the relative weights of the three orbitals [3, 6], this has not been observed in resonant x-ray scattering experiment [7] or LDA+SO+U calculation [8].

As the first approximation, the effective electronic Hamiltonian should be the projection of full Hamiltonian on the subspace of $J_{\text{eff}} = 1/2$ states. Considering first the Hamiltonian on the t_{2g} subspace, we expect the following, 1) the t_{2g} orbitals should be defined in the *local* cubic axis basis, because the crystal-field on Ir $5d$ orbitals from neighboring oxygens is diagonal only in the *local* cubic axis; 2) assuming that hoppings between Ir sites are mediated by the oxygen $2p$ orbitals, simple symmetry consideration shows that effective hoppings between nearest-neighbor Ir are orbital diagonal (one t_{2g} orbital does not hop to another orbital) only in the *local* cubic axis basis; 3) if the spin spaces are defined in the *global* axis basis, the effective hoppings of Ir t_{2g} orbitals will be real. Two tight-binding models on the t_{2g} subspace have been obtained by fitting LDA+SO+U dispersions in Ref. [8] and Ref. [13], and both have this property of real orbital diagonal hoppings, but no clear interpretation was given. The discussion above shows that the orbitals in these models should be interpreted as the t_{2g} orbitals in the *local* cubic axis, while the spins in these models are defined in the *global* axis.

The spin space on every site should be first rotated to *local* axis before the projection to the $J_{\text{eff}} = 1/2$ states, because the spins used in (2) are defined in local axis. Namely we need to interpret the electron operators $c_{j,a,\nu}^\dagger$ used in these models, on site j for orbital $a = XZ, YZ, XY$ with spin ν , as creation operators for the states $e^{i\epsilon_\nu \theta_j/2} |j, a, \nu\rangle$, where $\epsilon_\nu = \pm 1$ for spin index $\nu = \uparrow, \downarrow$ respectively.

Define d_\uparrow and d_\downarrow as the annihilation operators for the $|J_{\text{eff}}^z = \pm 1/2\rangle$ states (2) respectively. The projection on the $J_{\text{eff}} = 1/2$ subspace is implemented by the following substitution, $c_{j,XY,\nu}^\dagger \rightarrow -\epsilon_\nu \mathbf{i} \sqrt{1/3} e^{i\epsilon_\nu \theta_j/2} d_{j,\nu}^\dagger$, $c_{j,XZ,\nu}^\dagger \rightarrow \epsilon_\nu \sqrt{1/3} e^{i\epsilon_\nu \theta_j/2} d_{j,-\nu}^\dagger$, and $c_{j,YZ,\nu}^\dagger \rightarrow -\mathbf{i} \sqrt{1/3} e^{i\epsilon_\nu \theta_j/2} d_{j,-\nu}^\dagger$. The onsite interactions between t_{2g} orbitals will be projected into an onsite U term of the Hubbard model for the $J_{\text{eff}} = 1/2$ states due to time-reversal symmetry and charge conservation.

We take as a concrete example the tight-binding model of Ref. [13]. It involves nearest-neighbor (NN) XY hopping $t_1 = 0.36\text{eV}$, NN $XZ(YZ)$ hopping along $x(y)$ direction $t_4 = 0.37\text{eV}$, NN $XZ(YZ)$ hopping along $y(x)$ direction $t_5 = 0.06\text{eV}$, next-nearest-neighbor XY hopping $t_2 = 0.18\text{eV}$, and third-neighbor XY hopping $t_3 = 0.09\text{eV}$. The resulting one band Hubbard model after projection is

$$\begin{aligned} H = & - \sum_{\langle jk \rangle, \alpha} (t + \mathbf{i} \epsilon_\alpha \epsilon_j \bar{t}) d_{j,\alpha}^\dagger d_{k,\alpha} - \sum_{\langle\langle jk \rangle\rangle, \alpha} t' d_{j,\alpha}^\dagger d_{k,\alpha} \\ & - \sum_{\langle\langle\langle jk \rangle\rangle\rangle, \alpha} t'' d_{j,\alpha}^\dagger d_{k,\alpha} + U \sum_j d_{j,\uparrow}^\dagger d_{j,\uparrow} d_{j,\downarrow}^\dagger d_{j,\downarrow} \end{aligned} \quad (3)$$

with $\alpha = \uparrow, \downarrow$, and the effective hoppings are $t = (1/3)(t_1 + t_4 + t_5) \cos \theta \approx 0.258\text{eV}$, $\bar{t} = (1/3)(t_1 - t_4 - t_5) \sin \theta \approx -0.0045\text{eV}$, $t' = (1/3)t_2 \approx 0.06\text{eV}$, $t'' = (1/3)t_3 \approx 0.03\text{eV}$. \bar{t} is very small and will be ignored hereafter. In general \bar{t} can be absorbed into t by a unitary transformation $d_{j,\alpha} \rightarrow e^{i\epsilon_\alpha \epsilon_j \phi/2} \tilde{d}_{j,\alpha}$ with $\phi = \arctan(\bar{t}/t)$, but we will not elaborate on this. The value of U has been estimated as $\sim 2\text{eV}$ [8, 11]. This $t - t' - t'' - U$ model has been widely used as an effective model for the cuprates, although the parameters here have different values.

With large U and at half-filling the model (3) is an Mott insulator described by a pseudospin-1/2 model with $\text{SU}(2)$ symmetry. If second- and third-neighbor t', t'' are ignored the half-filling pseudospin model to the lowest order of t/U is just the Heisenberg AFM model of pseudospins \mathbf{J} , $H_{\text{AFM}} = \sum_{\langle jk \rangle} (4t^2/U) \mathbf{J}_j \cdot \mathbf{J}_k$. Each pseudospin has three components ($a = 1, 2, 3$) $J_{j,a} = (1/2) \sum_{\alpha, \beta} d_{j,\alpha}^\dagger (\sigma^a)_{\alpha\beta} d_{j,\beta}$, where σ are Pauli matrices and $\alpha, \beta = \uparrow, \downarrow$ label the $J_{\text{eff}}^z = \pm 1/2$ states.

Coupling to external magnetic field. Although the effective model (3) looks exactly like the model of the cuprates, the coupling to external magnetic field in Sr_2IrO_4 is quite different.

Assume the coupling of magnetic field \mathbf{B} on Ir $5d$ orbitals is described by the atomic form (more careful treatment can be found in, e.g., Ref. [6]), $H_B = -\mu_B \mathbf{B} \cdot (\mathbf{L} + 2\mathbf{S})$, where μ_B is the Bohr magneton. After projection to the $J_{\text{eff}} = 1/2$ states it becomes $H_B = 2\mu_B \mathbf{B} \cdot \mathbf{J} = 2\mu_B (B_X J_1 + B_Y J_2 + B_Z J_3)$. Note that $B_{X,Y,Z}$ are components of field on the *local* cubic axis, $B_X = \mathbf{B} \cdot \hat{X}$ etc.. Use the relation (1), the coupling on site j in terms of the field components on the global axis, B_x, B_y, B_z , is

$$H_{B,j} = 2\mu_B [B_{j,x}(J_{j,1} \cos \theta_j - J_{j,2} \sin \theta_j) + B_{j,y}(J_{j,2} \cos \theta_j + J_{j,1} \sin \theta_j) + B_{j,z} J_{j,3}] \quad (4)$$

Therefore the observable magnetic moment \mathbf{M}_j on site j has the following components on the global axis,

$$\begin{pmatrix} M_{j,x} \\ M_{j,y} \\ M_{j,z} \end{pmatrix} = -2\mu_B \begin{pmatrix} \cos \theta & -\epsilon_j \sin \theta & 0 \\ \epsilon_j \sin \theta & \cos \theta & 0 \\ 0 & 0 & 1 \end{pmatrix} \begin{pmatrix} J_{j,1} \\ J_{j,2} \\ J_{j,3} \end{pmatrix}. \quad (5)$$

If \bar{t} in (3) is not ignored $\theta \approx 11^\circ$ in (5) should be replaced by $\theta - \arctan(\bar{t}/t) \approx 12^\circ$. This nontrivial relation between moments \mathbf{M} and pseudospins \mathbf{J} , namely a g -tensor with a staggered antisymmetric component, has several interesting consequences which we list below.

i). By quantum Monte Carlo studies [14] the square lattice Heisenberg model has a Néel ground state with staggered “magnetization” $|\langle \epsilon_j \mathbf{J}_j \rangle| \approx 0.307$. However because of the relation (5), the ordered moments do not form a simple collinear Néel pattern. If the ordered moments lie in the xy plane, they will be rotated together with the oxygen octahedra in a staggered pattern therefore create a net ferromagnetic moment per site, $2\mu_B \cdot |\langle \epsilon_j \mathbf{J}_j \rangle| \cdot \sin \theta \approx 0.12\mu_B$. This is very close to the experimentally observed value $0.14\mu_B$ [12].

ii). By the relation (5) we can relate pseudospin correlation functions of model (3) to moment correlation functions which is actually measured by susceptibility or magnetic neutron/x-ray scattering experiments. The Fourier components of moments with wavevector \mathbf{q} and frequency ω is related to pseudospins by,

$$\begin{aligned} M_{\mathbf{q},\omega,x} &= -2\mu_B [\cos \theta J_{\mathbf{q},\omega,1} - \sin \theta J_{\mathbf{q}+\mathbf{Q},\omega,2}], \\ M_{\mathbf{q},\omega,y} &= -2\mu_B [\cos \theta J_{\mathbf{q},\omega,2} + \sin \theta J_{\mathbf{q}+\mathbf{Q},\omega,1}], \\ M_{\mathbf{q},\omega,z} &= -2\mu_B J_{\mathbf{q},\omega,3}. \end{aligned}$$

where $\mathbf{Q} = (\pi, \pi)$ is the wavevector of Néel order. In the paramagnetic phase the dynamical susceptibility $\chi^{ab}(\mathbf{q}, \omega)$, which is proportional to the “moment structure factor” $\langle M_{\mathbf{q},\omega,a} M_{-\mathbf{q},-\omega,b} \rangle$, is related to the dynamical pseudospin susceptibility $\chi_J^{ab}(\mathbf{q}, \omega) = \delta_{ab} \chi_J(\mathbf{q}, \omega) \propto \langle \mathbf{J}_{\mathbf{q},\omega} \cdot \mathbf{J}_{-\mathbf{q},-\omega} \rangle$ by

$$\begin{aligned} \chi^{xx}(\mathbf{q}, \omega) &= \chi^{yy}(\mathbf{q}, \omega) \\ &= \cos^2 \theta \chi_J(\mathbf{q}, \omega) + \sin^2 \theta \chi_J(\mathbf{q} + \mathbf{Q}, \omega), \end{aligned}$$

$\chi^{zz}(\mathbf{q}, \omega) = \chi_J(\mathbf{q}, \omega)$, and other components of χ^{ab} are zero. In particular the measured static uniform ($\omega = 0, \mathbf{q} = 0$) susceptibility in xy plane is actually a mixture of the uniform and staggered susceptibility of the SU(2) invariant Hubbard/Heisenberg model. This explains in a different perspective the measured large anisotropy of uniform susceptibility and the ferromagnetic Curie-Weiss law [12]. In our picture the anisotropy is not mainly from easy axis interaction suggested by Ref. [12] but from the mixing of large staggered susceptibility, and the FM Curie-Weiss law comes from the contribution of staggered susceptibility close to AFM Néel order of pseudospins.

iii). In the high temperature paramagnetic phase above the Néel ordering temperature, the measured moment-moment correlation will be dominated by the staggered pseudospin correlation of a SU(2) invariant model, although the measured susceptibility shows significant anisotropy. The moment-moment correlation length will behave like the 2D Heisenberg model [15], which has recently been observed by magnetic x-ray scattering [16].

Possible high-temperature superconductivity.

If the one band Hubbard model (3) is indeed a good approximation of the electronic structure of Sr_2IrO_4 , and if the high-temperature superconductivity in doped cuprates is indeed described by the one band Hubbard model, a natural consequence is that doped Sr_2IrO_4 will realize high-temperature superconductivity. In the following we list several direct consequences from this analogy.

i). It is believed that the sign and magnitude of t' is important for high-Tc in the cuprates and likely responsible for the particle-hole asymmetry of the phase diagram. (see e.g., Ref. [17]). The relative magnitude $|t'/t| \approx 0.23$ for Sr_2IrO_4 is similar to the cuprates. However the sign of t' for Sr_2IrO_4 is opposite to that of the cuprates. This can be remedied by a particle-hole transformation $d_{j,\alpha} \rightarrow \epsilon_j d_{j,\alpha}^\dagger$. Therefore we expect that the doping phase diagram of Sr_2IrO_4 will be the particle-hole conjugate of the cuprates, in particular high-Tc will be easier to achieve on the electron-doped side of Sr_2IrO_4 , e.g. with La substitution of Sr. Interestingly electron-doped $\text{Sr}_2\text{IrO}_{4-\delta}$ has recently been synthesized and metallic behavior was reported for $\delta = 0.04$ [18].

ii). The interlayer hopping of the cuprates is of the form $t_\perp(k_\parallel) = t_{\perp 0} v^2$ with $v = (\cos k_x - \cos k_y)/2$, due to the $d_{x^2-y^2}$ orbital content [19]. This together with the $d_{x^2-y^2}$ nodal pairing symmetry significantly suppress transport along c -axis, making the superconducting properties of the cuprates very anisotropic. However the resistivity anisotropy ρ_c/ρ_{ab} of Sr_2IrO_4 is only $10^2 - 10^3$ [20], very small compared to $10^4 - 10^5$ of the cuprates [21], which implies a larger $t_{\perp 0}$ for Sr_2IrO_4 . The active orbitals for Sr_2IrO_4 is very different from the cuprates and the factor v^2 should be different and not vanish on the nodal direction. Both facts suggest that Sr_2IrO_4 should

have more isotropic superconducting properties which is beneficial for practical applications.

iii). The pairing will be a pseudospin singlet $d_{x^2-y^2}$ pairing and in many ways behave like the d-wave pairing of the cuprates. Phase sensitive and other indirect measurements used to determine the d-wave symmetry in the cuprates can be applied to doped Sr_2IrO_4 as well.

iv). The energy scale of the one band Hubbard model for Sr_2IrO_4 is lower than that of the cuprates by about 50%. Therefore the T_c of doped Sr_2IrO_4 will likely be lower than the cuprates.

Discussion and Conclusion. The one band Hubbard model (3) is of course the zeroth order approximation of the low energy electronic structure of Sr_2IrO_4 . Indeed there are experimental and theoretical evidences [8, 11, 13] that the $J_{\text{eff}} = 3/2$ bands overlap with the $J_{\text{eff}} = 1/2$ band and therefore strong exchange anisotropy might be present. However the observed scaling of correlation length follows that of isotropic Heisenberg model above Néel temperature [16], and the $J_{\text{eff}} = 3/2$ bands are completely below Fermi level for about 0.3eV from ARPES results [11]. We thus believe that for magnetic properties above the Néel temperature and for *electron-doped* Sr_2IrO_4 this SU(2) invariant one band Hubbard model is still a good description.

The projection to one band Hubbard model was also implemented in Ref. [8]. The resulting hoppings reported in Equ. (7)(8) of Ref. [8] suggest that the authors of Ref. [8] interpreted the orbitals in their t_{2g} tight-binding model as the *global* axis basis xz, yz, xy . Here we have argued that the orbitals should be interpreted as the *local* axis basis which produces a projection result [$\bar{t}_0 = -(2t_0/3) \cos\theta$ and $\bar{t}_1 = 0$] different from Ref. [8].

In summary we have performed the projection of the electronic structure of Sr_2IrO_4 to the $J_{\text{eff}} = 1/2$ states and carefully deduced the resulting one band Hubbard model and its interpretation. We provide another perspective on the magnetic properties of Sr_2IrO_4 by viewing it as a SU(2) invariant Hubbard/Heisenberg pseudospin-1/2 model, but with a twisted relation (5) between the observable moments and the pseudospin degrees of freedom, namely a g -tensor with staggered antisymmetric component. One direct consequence is that the measured uniform susceptibility in ab plane is actually a mixture of uniform and staggered susceptibility of SU(2) invariant Hubbard/Heisenberg model. Despite the complication of strong SO interaction, different active orbitals and structure distortion, the effective one band Hubbard model of Sr_2IrO_4 remarkably resembles the cuprates. We thus propose that doped Sr_2IrO_4 can realize high-temperature superconductivity, and potentially other interesting physics of the cuprates. By comparing the model parameters we suggest that electron-doping of Sr_2IrO_4 will be the analogue of hole-doping of the cuprates. This can be achieved by La substitution of Sr, or O deficiency [18], and maybe by field effect on thin films [22], or interfacing

with other oxides [23]. We hope these simple theoretical observations will stimulate more experimental research on Sr_2IrO_4 .

Acknowledgment The authors thank Leon Balents, Dung-Hai Lee, Patrick A. Lee, and Michael Norman for helpful discussions. TS was supported by NSF through the grant DMR-1005434.

-
- [1] Y. Okamoto, M. Nohara, H. Aruga-Katori, and H. Takagi, *Phys. Rev. Lett.* **99**, 137207 (2007).
- [2] A. Shitade, H. Katsura, J. Kuneš, X.-L. Qi, S.-C. Zhang, and N. Nagaosa, *Phys. Rev. Lett.* **102**, 256403 (2009); D. A. Pesin, and Leon Balents, *Nat. Phys.* **6**, 376 (2010) Bohm-Jung Yang, and Yong Baek Kim, *Phys. Rev. B* **82**, 085111 (2010).
- [3] G. Jackeli, and G. Khaliullin, *Phys. Rev. Lett.* **102**, 017205 (2009).
- [4] Xiangang Wan, A. M. Turner, A. Vishwanath, and S. Y. Savrasov, arXiv:1007.0016 (2010).
- [5] M. K. Crawford, M. A. Subramanian, R. L. Harlow, J. A. Fernandez-Baca, Z. R. Wang, and D. C. Johnston, *Phys. Rev. B* **49**, 9198 (1994); Q. Huang, J. L. Soubeyroux, O. Chmaissem, I. Natali Sora, A. Santoro, R. J. Cava, J. J. Krajewski, and W. F. Peck, Jr., *J. Sol. St. Chem.* **112**, 355 (1994).
- [6] B. Bleaney, and M. C. M. O'Brien, *Proc. Phys. Soc. B* **69**, 1216 (1956).
- [7] B. J. Kim, H. Ohsumi, T. Komesu, S. Sakai, T. Morita, H. Takagi, T. Arima, *Science* **323**, 1329 (2009).
- [8] H. Jin, H. Jeong, T. Ozaki, and J. Yu, *Phys. Rev. B* **80**, 075112 (2009).
- [9] R. J. Cava, B. Batlogg, K. Kiyono, H. Takagi, J. J. Krajewski, W. F. Peck, Jr., L. W. Rupp, Jr., and C. H. Chen, *Phys. Rev. B* **49**, 11890 (1994).
- [10] S. J. Moon, M. W. Kim, K. W. Kim, Y. S. Lee, J.-Y. Kim, J.-H. Park, B. J. Kim, S.-J. Oh, S. Nakatsuji, Y. Maeno, I. Nagai, S. I. Ikeda, G. Cao, and T. W. Noh, *Phys. Rev. B* **74**, 113104 (2006).
- [11] B. J. Kim, Hosub Jin, S. J. Moon, J.-Y. Kim, B.-G. Park, C. S. Leem, Jaejun Yu, T.W. Noh, C. Kim, S.-J. Oh, J.-H. Park, V. Durairaj, G. Cao, and E. Rotenberg, *Phys. Rev. Lett.* **101**, 076402 (2008).
- [12] G. Cao, J. Bolivar, S. McCall, J. E. Crow, and R. P. Guertin, *Phys. Rev. B* **57**, 11039(R) (1998).
- [13] H. Watanabe, T. Shirakawa, and S. Yunoki, *Phys. Rev. Lett.* **105**, 216410 (2010).
- [14] J. D. Reger, and A. P. Young, *Phys. Rev. B* **37**, 5978 (1988); A. W. Sandvik, *Phys. Rev. B* **56**, 11678 (1997).
- [15] S. Chakravarty, B.I. Halperin, D.R. Nelson, *Phys. Rev. B* **39**, 2344 (1989); M.S. Makivić, H.-Q. Ding, *Phys. Rev. B* **43**, 3562 (1991).
- [16] Shigeaki Fujiyama, presentation in the “Highly Frustrated Magnetism 2010” conference, August 2010 (unpublished).
- [17] P. A. Lee, N. Nagaosa, and X.-G. Wen, *Rev. Mod. Phys.* **78**, 17 (2006).
- [18] O.B. Korneta, Tongfei Qi, S. Chikara, S. Parkin, L. E. De Long, P. Schlottmann, and G. Cao, *Phys. Rev. B* **82**, 115117 (2010).
- [19] O. K. Anderson, A. I. Liechtenstein, O. Jepsen, and F. Paulsen, *J. Phys. Chem. Solids* **56**, 1573 (1995).
- [20] S. Chikara, O. Korneta, W. P. Crummett, L. E. DeLong, P. Schlottmann, and G. Cao, *Phys. Rev. B* **80**, 140407(R) (2009).
- [21] S. Martin, A. T. Fiory, R. M. Fleming, L. F. Schneemeyer, and J. V. Waszczak, *Phys. Rev. B* **41**, 846 (1990).
- [22] J. T. Ye, S. Inoue, K. Kobayashi, Y. Kasahara, H. T. Yuan, H. Shimotani, and Y. Iwasa, *Nat. Mat.* **9**, 125 (2010).
- [23] J. Mannhart, and D. G. Schlom, *Science* **327**, 1607 (2010).